MJ-66 induces malignant glioma cells G2/M phase arrest and mitotic catastrophe through regulation of cyclin B1/Cdk1 complex

Wei-Ting Liu[a], **Ching Chen**[a], **I-Chen Lu**[a], **Sheng-Chu Kuo**[b], **Kuo-Hsiung Lee**[c,d], **Tai-Lin Chen**[e], **Ta-Shu Song**[e], **Yi-Liang Lu**[e], **Po-Wu Gean**[a,**], and **Mann-Jen Hour**[e,f,*]

[a]Department of Pharmacology, College of Medicine, National Cheng-Kung University, Tainan, Taiwan

[b]Graduate Institute of Pharmaceutical Chemistry, China Medical University, Taichung, Taiwan

[c]Natural Products Research Laboratories, UNC Eshelman School of Pharmacy, University of North Carolina at Chapel Hill, NC 27599, USA

[d]Chinese Medicine Research and Development Center, China Medical University and Hospital, Taichung, Taiwan

[e]School of Pharmacy, China Medical University, Taichung, Taiwan

[f]China Medical University Hospital, Taichung, Taiwan

Abstract

Malignant gliomas are among the most devastating cancers as they are resistant to many kinds of treatment. Despite recent advances in the diagnosis and treatment, the prognosis of patients remains very poor and the development of new drug is urgently needed. Here, we report that a synthetic quinazolinone analog 2-(naphthalene-1-yl)-6-pyrrolidinyl-4-quinazolinone (MJ-66) induced glioma cell death. Immunofluorescence staining showed that MJ-66-induced cell death was associated with multinucleated phenotype and multipolar spindles that were typical characteristics of mitotic catastrophe. Flow cytometry analysis revealed that MJ-66 caused glioma cell cycle arrest at G2/M phase and increased the proportion of polyploidy cells. Western blotting indicated that the expression of cyclin B1, Cdk1 pY15 and Cdk1 increased after treatment with MJ-66. MJ-66 effectively inhibited tumor growth and induced apoptosis in the xenograft animal model of U87 human glioma cells. Together, these results suggest that MJ-66 inhibited malignant gliomas growth through inducing mitotic catastrophe by interference with G2/M cell cycle checkpoint which may open a new avenue for the treatment of malignant gliomas.

Keywords

Malignant glioma; 2-(Naphthalene-1-yl)-6-pyrrolidinyl-4-quinazolinone; Mitotic catastrophe; G2/M arrest; Xenograft animal model

*Corresponding author. School of Pharmacy, China Medical University, 91, Hsueh-Shih Road, Taichung 40402, Taiwan. Tel.: +886 4 22053366x5123. **Corresponding author. Tel.: +886 6 2353535x5507; fax: +886 6 2749296.

1. Introduction

Mitosis is a process of cell division in which a eukaryotic cell separates the chromosomes in its cell nucleus into two identical sets, in two separate nuclei resulting in the production of two daughter cells. The daughter cells are identical to one another and to the original parent cell. During mitosis the pairs of chromatids condense and attach to fibers that pull the sister chromatids to opposite sides of the cells. The cell then divides in cytokinesis, to produce two identical daughter cells which are still diploid cells (Maton et al., 1997; De Souza and Osmani, 2007). Mitotic catastrophe (MC) has been widely used as a mode of cell death that results from unscheduled activation of cyclin B1–CDK1, premature or inappropriate entry of cells into mitosis and can be caused by chemical or physical stresses (Castedo et al., 2004a,b; Vakifahmetoglu et al., 2008; Vitale et al., 2011). Mitotic catastrophe occurs either during or shortly after abnormal mitosis and is accompanied by the formation of giant micronucleated cells, which reflects the abnormal segregation of chromosomes (Fukasawa, 2007; Kroemer et al., 2009). It has been shown that increased expression of cyclin B1 and Cdk1 or inhibition of DNA repair regulatory protein (such as ATR, ATM, Chk1, Chk2, Plk and 14-3-3ρ) as well as defective spindle assembly regulators (such as Mad, Bub, Survivin, Aurora B kinase) and anaphase promoting complex can cause mitotic catastrophe (de Bruin and Medema, 2008). Since mitotic catastrophe also resulted in caspase activation, chromatin condensation, mitochondrial release of pro-apoptotic proteins (cytochrome c or AIF) and DNA fragmentation (Castedo et al., 2004a,b), previous studies suggested that mitotic catastrophe was followed by apoptosis (Chakrabarti and Chakrabarti, 1987; Heald et al., 1993; Jordan et al., 1996; Merritt et al., 1997; Vakifahmetoglu et al., 2008). However, some studies suggest that mitotic catastrophe is a cell characteristic that is distinct from apoptosis (Lock and Stribinskiene, 1996; Roninson et al., 2001; Broker et al., 2005; Fragkos and Beard, 2011).

Although the prevalence of malignant glioma is relatively low compared with other cancers such as lung, breast, prostate, colorectal, and liver cancers, malignant gliomas are among the most devastating cancers as they are resistant to many kinds of treatment. Malignant gliomas are normally treated with neurosurgery, followed by radiotherapy and chemotherapy with temozolomide (TMZ). However, TMZ therapy produces only modest increase in survival so that the development of new drugs for the treatment of malignant gliomas is urgently needed. TMZ is a cytotoxic imidazotetrazine that leads to the formation of O^6-methylguanine, which mismatches with thymine in subsequent DNA replication cycles. This induced apoptosis, autophagy mitotic catastrophe and senescence-like events in glioma cells (Hirose et al., 2001; Hermisson et al., 2006).

Quinazolinone is a heterocyclic compound and quinazolinone analogs possess diverse pharmacological activity, including anti-bacterial, anti-viral, anti-fungal, anti-malarial, anti-inflammation, anti-depressant, anti-hypertensive and anti-cancer effects (Chinigo et al., 2008; Hour et al., 2000; Li et al., 2010; Marzaro et al., 2012). These compounds interfered with DNA repair pathway, cytoskeleton, and cell proliferation in lung, liver, and colon cancer cells (Cao et al., 2006; Giri et al., 2010; Wu et al., 2011). In the present study, we investigated the effect of synthetic quinazolinone compounds, 2-(naphthalene-1-yl)-6-

pyrrolidinyl-4-quinazolinone (MJ-66), 6-(piperidin-1-yl)-2-(naphthalen-1-yl)quinazolin-4-one (MJ-68) and 6-(pyrrolidin-1-yl)-2-(benzo[b]thiophen-3-yl)quinazolin-4-one (MJ-78), on malignant glioma cells. We found that MJ-66-induced cell death was associated with multinucleated phenotype and multipolar spindles that are typical characteristics of mitotic catastrophe. MJ-66 effectively inhibited tumor growth and induced apoptosis in the xenograft animal model of U87 human glioma cells. Thus, MJ-66 seems to be a promising agent for the treatment of malignant gliomas.

2. Materials and methods

2.1. Cell culture and reagents

The human glioma cell lines U87, U251, T98G, U373, and rat glioma cell line RT2 provided by Dr. Michael Hsiao (Genomics Research Center, Academia Sinica, Taiwan) were cultured in Dulbecco's Modified Eagle medium (DMEM, Caisson) supplemented with 10% fetal bovine serum (FBS, Sigma–Aldrich), 2 mM L-glutamine (Caisson), 100 U/ml penicillin, and 0.1 mg/ml streptomycin (Caisson). The rat glioma C6 cell line provided by Dr. Shun-Fen Tzeng (National Cheng Kung University, Taiwan) was cultured in DMEM/F12 (Caisson) supplemented with 10% fetal bovine serum, 2 mM L-glutamine, 100 U/ml penicillin, and 0.1 mg/ml streptomycin. The human normal glia cell line SVGP12, kindly provided by Dr. Michael Hsiao was cultured in Minimum Essential Medium (MEM, Invitrogen) supplemented with 10% fetal bovine serum, 2 mM L-glutamine, 100 U/ml penicillin, and 0.1 mg/ml streptomycin. Primary glia cells were prepared by surgery. Cerebral cortices without meninges were dissected from postnatal (P_0–P_2) Sprague–Dawley (SD, NCKU Laboratory Animal Center) rats and dissociated in 0.05% trypsin-EDTA (Biowest) at 37 °C for 10 min. Add culture medium and pipette several times, and remove supernatant after centrifuged at 1000 rpm for 5 min, glia cells were filtered through 70 μm cell strainer (BD Falcon) and then cultured in Neuralbasal A medium (Gibco) supplemented with 5% fetal bovine serum (Sigma–Aldrich), 2 mM L-glutamine, 100 U/ml penicillin, 0.1 mg/ml streptomycin and 17.5 mM D-glucose on 50 μg/ml poly-D-lysine (Sigma–Aldrich) pre-coating dish. All cells were maintained in a humidified incubator at 37 °C and 5% CO_2/95% air. MJ-66, MJ-68 and MJ-78 provided by Dr. Mann-Jen Hour (China Medical University, Taiwan) (Hour et al., 2013) were dissolved in dimethylsulfoxide (DMSO) as stock solution at concentration of 1 mM.

2.2. Cell proliferation and viability assay

2.2.1. MTS assay—Cell proliferation was determined by MTS (tetrazolium compound 3-(4, 5-dimethylthiazol-2-yl)-5-(3-carboxymethoxyphenyl)-2-(4-sulfophenyl)-2H-tetrazolium) assay (Promega). MTS assay is a colorimetric assay for determining cell viability (Mosmann, 1983). The MTS tetrazolium compound is bio-reduced by NADPH or NADH produced by dehydrogenase in live cells into a colored formazan product. Cells were seeded in 96-well plates (C6, U87, U251, U373, T98G, 2000/well; RT2, 1000/well; SVGP12, primary glia cells, 5000/well) for MTS assay and cells were incubated for 24 h. Culture medium containing sequential concentration MJ-66, MJ-68 and MJ-78 (1, 0.1, 0.05, 0.025, 0.0125, 0.00625 μM) or DMSO (0.1%) was added to each well, and cells were incubated at 37 °C. At the indicated time points (0, 24.48,72 h), medium were removed, and then fresh

culture medium (100 μl/well) with MTS solution (20 μl/well) were added, and cells were incubated at 37 °C for 1–4 h. The absorbance of soluble formazan was measured at 490 nm with microplate reader (Molecular device). The cell viability was determined by the percentage of the absorption relative to untreated control.

2.2.2. Trypan-blue exclusion assay—Cell viability was also determined by trypan-blue exclusion assay (Sigma). Cells were seeded in 6-well plates (2×10^4/well) for trypan blue exclusion assay, and incubated for 24 h at 37 °C. Culture medium containing MJ-66 (IC_{50}) or DMSO (0.006%) was added to each well, and cells were incubated at 37 °C. At indicated time points (0, 24, 48, 72, 96 h), cells were suspended with 0.05% trypsin-EDTA, and stained with trypan-blue dye (0.4%). The cell viability was evaluated by the percentage of death relative to the total cell, and cell growth curve was determined by live cell relative to the total number of cells.

2.3. Flow cytometry

2.3.1. Cell cycle assay—To analyze cellular DNA content by flow cytometry, 3×10^5 cells were seeded in 10 cm dish and incubated for 24 h at 37 °C. Culture medium containing MJ-66 (IC_{50}) or DMSO (0.006%) was added, and cells were incubated for 24 h at 37 °C. At indicated time points (0, 6, 12, 24, 48 h), $>10^6$ cells were suspended with 0.05% trypsin-EDTA, and fixed in 70% ethanol > 1 h at −20 °C. After washed by phosphate-buffered saline (PBS) twice, cells were then suspension with 1 ml propidium iodide/Triton-X 100 staining solution (20 μg/ml PI, 0.1% Triton-X 100, 0.2 mg/ml ribonuclease A (RNase A, Sigma) in PBS) and incubate 30 min at room temperature in the dark. After filtered by 35 μm nylon mesh (Falcon, 352235), the DNA content was then analyzed by flow cytometry (FACS can, BD Bioscience). The cell-cycle distribution (subG1, G1, S, G2/M, and >4N DNA content) of ten thousand cells was analyzed by WinMDI software.

2.3.2. G1 synchronized by Ara-C—To analyze the effect of cytosine arabinoside (Ara-C, a DNA synthesis inhibitor) on the MJ-66-treated glioma cells by flow cytometry. After seeded 3×10^5 cells in 10 cm plate for at least 24 h at 37 °C, glioma cells were then treated with Ara-C (4.17 mM/ml) for 12 h, and then MJ-66 (IC_{50}) or DMSO (0.006%) was added. At indicated time points (0, 6, 12, 24 h), $>10^6$ cells were collected and fixed in 70% ethanol > 1 h at −20 °C. After staining with PI as described, DNA content of ten thousand cells was analyzed by flow cytometry.

2.3.3. Annexin V-FITC/PI staining—To evaluate whether MJ-66-treated glioma cells cell death undergo apoptosis or necrosis by flow cytometry. Annexin V-FITC/PI staining (Andree et al., 1990; Casciola-Rosen et al., 1996) was performed to detect early or late apoptosis. Translocation of phosphatidylserine (PS) on the outer membrane that disrupt membrane asymmetry of membrane is a characteristic in early apoptosis that cell membrane remains intact. Annexin V has a highly binding affinity to exposure PS, thus annexin V was used to detect the early apoptotic cells. 3×10^5 cells were seeded in 10 cm plate and incubated at least 24 h at 37 °C. Glioma cells were treated with medium containing MJ-66 (IC_{50}) or DMSO (0.006%), and incubated at 37 °C. At indicated time points (24, 36, 48 h), cells were suspended with 0.05% trypsin-EDTA, and 1×10^5 cells were stained with

Annexin V-FITC (5 μl, BD Bioscience) and PI (5 μg/ml). The percentage of the apoptotic or necrotic cells (intact cell, FITC$^-$/PI$^-$; early apoptotic cell, FITC$^+$/PI$^-$; late apoptotic or necrotic cell, FITC$^+$/PI$^+$) was then detected by flow cytometry. Apoptotic cells (FITC$^+$/PI$^-$) were counted and represented as percentage of the total cell count.

2.4. Immunofluorescent staining

2×10^4 cells were seeded on the PDL-coating 12 mm glass coverslips in 24-well plate and allowed to attach for 24 h at 37 °C. Culture medium containing MJ-66 (IC$_{50}$) or DMSO (0.006%) was added, and cells were incubated at 37 °C. At indicated time points (0, 12, 24 h), cells were fixed in 4% paraformaldehyde (PFA) in PBS for 30 min. After permeabilized by 0.2% Triton X-100 in 0.1 M PBS for 10 min and 10% methanol containing 0.2% Triton X-100 in 0.1 M PBS for 5 min, cells were blocked in 3% bovine serum albumin (BSA, Sigma) for 1 h. The cells were immunostained for mitotic spindle with mouse monoclonal alpha-tubulin (Sigma–Aldrich), and mitotic center with rabbit polyclonal gamma-tubulin (Genetex), and then stained with appropriated secondary antibodies conjugated with Texas Red or FITC for 1 h. Nuclei were stained with Hoechst 33342 for 10 min (0.5 μg/ml, Sigma–Aldrich, B2261). Fluorescence images were detected by confocal laser scanning microscope (FV1000, Olympus).

2.5. Western blotting assay

To evaluate the mechanisms in MJ-66-treated glioma cells cell death by Western blot, 3×10^5 cells were seeded in 10 cm plate and incubated at least 24 h at 37 °C. Glioma cells were treated with medium containing MJ-66 (IC$_{50}$) or DMSO (0.006%), and incubated at 37 °C. At indicated time points (0, 12,18, 24, 48 h), cells pellets were collected and centrifuged at 4000 rpm and stored at −80 °C. Cell pellets were lysed in a RIPA lysis buffer containing 50 mM Tris–HCl, pH 7.4, 150 mM NaCl, 1% Nonidet P-40, 0.25% sodium deoxycholate, 0.1% SDS with complete protease inhibitor cocktail (Roche). Lysates were shaken at 30 rpm on ice for 1 h and then centrifuged at 13,000 rpm for 30 min. Supernatants were collected and determined concentration, subjected to heated in 5× sample buffer (12.5 mM Tris, 25% glycerol, 4% SDS, 1.54% DTT and 0.02% Bromophenol blue) at boiled-water for 10 min. Protein electrophoresis on 12%, 10%, or 8.5% SDS-polyacrylamide gel under 120 V, and the separated protein was transferred to a PVDF membrane (Immunobilon transfer membranes, Millipore) by semi-dry transfer system (BIO-RAD) under 400 mA, 20 V for 1.5 h. The membrane was then immersed in 5%-TBST nonfat milk for 60 min at room temperature to perform non-specific blocking, and then reacted with the following primary antibodies: rabbit polyclonal Caspase-2 (Abcam), rabbit polyclonal Caspase-3 (Cell signaling), mouse monoclonal actin (Sigma, U.S.A), mouse monoclonal Chk1 (Gentex), mouse monoclonal Cdc2 (Genetex), rabbit polyclonal Chk2 phospho T68 (Abcam), mouse monoclonal Chk2 (BD Transduction Laboratories), rabbit polyclonal Cdc2 phospho T161 (Abcam), polyclonal mouse Cdc2 phospho Y15 (BD Transduction Laboratories), mouse monoclonal Cyclin B1 (Millipore), rabbit polyclonal BAD phosphor S112, rabbit monoclonal BAD (Epitomics) or rabbit monoclonal Laminin (Cell signaling) at 4 °C overnight. The membrane was washed with TBST 3 times, and HRP-labeled secondary antibody (Jackson ImmunoResearch Lab., USA) was used at 1:10,000 concentrations and incubated at room temperature for 1 h. After washed with TBST for three times on shaker at

50 rpm, the ECL-plus chemical reagents (PerkinElmer) were added to the membrane and incubated for 1 min. Films (Fuji, Japan) were exposed at different time points to ensure the optimum density, but not saturated. The resulting Western blots were analyzed for desitometrically by using ImageJ software. Three replicates were performed for each experiment.

2.6. In vivo xenograft animal model

The male nude mice (8–10 weeks old, BALB/cAnN-Foxnlnu/CrlNarl mice) were obtained from Laboratory Animal Centre (LAC) of National Cheng Kung University (Tainan, Taiwan). All animals were housed in light- and temperature-controlled environments with food and water available ad libitum. All animal experiments were reviewed and approved by the Institutional Animal Care and Use Committee (IACUC) of National Cheng Kung University. For tumorigenesis, U87 glioma cells (1×10^6 cells per l00 µl PBS) were inoculated subcutaneously into the right flank of mice. Tumor growth was measured every three days. Tumor volume was calculated by volume (mm^3) = (length $\times$ width^2)/2 (Zhou et al., 2005). When the tumors reached a mean volume of 50–70 mm^3, MJ-66 (1.36 µg/kg in saline) or vehicle (DMSO or saline) were injected intratumor once per two days for 20 days.

2.7. Statistical analysis

Experiments were performed at least in triplicate. All results were expressed as the mean $\pm$ standard error of the mean. Independent experiments were analyzed by unpaired t test. Levels of $P < 0.05$ were considered to be of statistical significance.

3. Results

3.1. MJ-66, MJ-68 and MJ-78 induced glioma cell death

Fig. 1A shows the structures of 4-quinazolinone analogs. To investigate the effects of quinazolinone analogs on cell proliferation, C6 and U87 glioma cells were treated with various concentrations of MJ-66, MJ-68, or MJ-78 for 48 h and cell viability was measured by MTS assay. As shown in Fig. 1B, cell viability was concentration-dependently inhibited by MJ-66 with median inhibitory concentrations (IC_{50}s) of 0.06 ± 0.15 µM and 0.05 ± 0.013 µM for C6 and U87 cells respectively. The IC_{50}s of MJ-68 for C6 and U87 glioma cells were 0.47 ± 0.165 µM and 0.57 ± 0.24 µM respectively. By contrast, MJ-78 was much less effective with $IC_{50} > 1$ µM for both C6 and U87 glioma cells (Table 1). Since MJ-66 was the most potent compound, we further investigated its concentration- and time-dependent effects on rat glioma cell lines of C6 and RT2, and human glioma cell lines of U87, U251, U373 and T98G (Fig. 1C). Table 2 shows the IC_{50}s of MJ-66 on these cells. C6 and U87 glioma cells were treated with MJ-66 (30, 60, 90 nM) or vehicle (DMSO, 0.009%) for 48 h and morphological changes were observed including cell rounding and shrinkage (Fig. 1D).

3.2. MJ-66 caused C6 glioma cells G2/M arrest

We investigated the effect of MJ-66 on the cell cycle distribution. C6 glioma cells, treated with 60 nM MJ-66 for the indicated time, were stained with propidium iodide (PI) and cell cycle distribution was monitored by flow cytometry. FACS analysis revealed that 6–12 h of MJ-66 treatment significantly increased the percentage of cells in the G2/M phase (Fig. 2A).

In addition, 12 h after MJ-66 treatment, the percentage of cells in the sub-G1 phase and with DNA content >4N were significantly increased (Fig. 2B). These data suggest that MJ-66 induces glioma cell death early through G2/M arrest and mitotic catastrophe, and later apoptosis.

To investigate the influence of MJ-66 on normal glia such as human glia cell line SVGP12 and rat primary glia cells, cells were treated with different concentrations of MJ-66 and viability was assessed by MTS assay (Fig. 3A). Cell viability of SVGP12 and rat glia cells was inhibited by MJ-66 with IC_{50}s of 0.06 μM and 0.04 μM respectively. Since glia cells proliferate constantly *in vitro*, we tested the possibility that proliferating cells were more sensitive to MJ-66 by pre-treating glia cells with cytosine arabinoside-C (Ara-C), a DNA synthesis inhibitor which inhibited proliferation. Then the cells were treated with MJ-66, stained with PI and analyzed by flow cytometry. Fig. 3C shows that MJ-66 did not induce cell death in Ara-C-pretreated glia cells. These results suggest that proliferating cells were more sensitive to MJ-66 than those of non-proliferating glia cells.

3.3. MJ-66 induces glioma cell death through apoptosis but not necrosis

Given that MJ-66 induced cell death in glioma cells by interfering with cell cycle, we determined whether it was due to apoptosis or necrosis. Fig. 4A shows that activation of caspase-2 (cleaved caspase-2) and caspase-3 (cleaved caspase-3) increased dramatically after treatment of MJ-66 for 24 or 48 h suggesting that glioma cells underwent apoptosis. Next, glioma cells were treated with MJ-66 for various times and co-stained with early-apoptotic marker Annexin V-FITC and necrotic marker PI. PI is a nonspecific DNA intercalating agent, which is excluded by the plasma membrane of living cells, and thus can be used to distinguish necrotic cells from apoptotic. FACS analysis revealed that the percentage of FITC$^+$/PI$^-$ cell population increased in a time-dependent manner (Fig. 4B). Thus, MJ-66 induces cell death through caspase-dependent apoptosis, but not necrosis. However, as noted in Fig. 4B, only 24.6% cells underwent late apoptosis in comparison with about 50% cell death induced by 60 nM MJ-66. Taken together, these results suggest that MJ-66 induced G2/M arrest and mitotic catastrophe cell death, and caspase-dependent apoptotic cell death.

3.4. MJ-66-induced multinucleated phenotype and multipolar spindles in glioma cells

Glioma cells were treated with MJ-66 for 24 h, stained with Hoechst 33342 and antibodies against α-tubulin conjugated with FITC, and then detected with confocal laser scanning microscope. Fluorescence images showed that glioma cells treated with MJ-66 exhibited abnormal nuclear phenotype and possessed multinuclear giant cells (Fig. 5A). In the early stage, we also discovered that MJ-66-treated cells with aberrant multipolar spindle and unaligned chromosomes (Fig. 5B). The formation of multinuclear and multipolar spindle is a typical characteristic of mitotic catastrophe.

3.5. MJ-66 increases Cdk1/cyclin B1 activity in C6 glioma cells

Cdk1/cyclin B1 complex, the critical target of G2/M checkpoint, plays critical roles in mitosis and mitotic catastrophe (Castedo et al., 2004a,b). We used Western blot analysis to investigate the expression of cyclin B1, Cdk1 pY15 and Cdk1 after treatment with MJ-66.

As shown in Fig 6, the expression of cyclin B1 increased at 6, 12 and 18 h after the treatment with MJ-66 and then returned to baseline at 24 h. The expression of inhibitory Cdk1 pY15 increased at 6 h after the treatment with MJ-66 and then returned to baseline at 12 h. The expression of Cdk1 had a similar time course as the expression of cyclin B1. Accordingly, MJ-66-induced glioma mitotic catastrophe was mediated through interrupting with cyclin B1/Cdk1 complex activity. We next determined the phosphorylated level of BAD at Ser112. BAD. As illustrated in Fig. 6C and D, phosphorylated level of BAD decreased after 12–24 treatment of MJ-66 (60 nM).

3.6. MJ-66 inhibits tumor growth in a xenograft animal model

We examined whether MJ-66 inhibited tumor growth in a U87 human glioma xenograft animal model. Nude mice were inoculated subcutaneously with 1×10^6 U87 glioma cells. When tumors reached 50–70 mm^3 in volume, MJ-66 (1.36 μg/kg in saline) or saline were injected into the tumor every 2 days for 10 times and tumor growth was observed for 20 days after the cessation of treatment. Tumor growth was significantly inhibited by MJ-66 (tumor volume, Control: 2234 ± 214.2 mm^3, $n = 8$; vehicle: 1894 ± 148.9 mm^3, $n = 9$; MJ-66: 944.7 ± 92.3 mm^3, $n = 8$, $p < 0.01$, MJ-66 vs. control and vehicle) (Fig. 7). To examine whether MJ-66 induced apoptosis in vivo, we examined the activation of caspase-3, especially the cleavage of caspase-3. As shown in Fig. 7C, the cleavage of caspase-3 increased significantly in tumors treated with MJ-66.

4. Discussion

In the present study, we demonstrated that MJ-66 induced cell death in C6 and U87 glioma cells in a concentration-dependent manner with IC$_{50}$s of approximately 0.06 ± 0.15 μM and 0.05 ± 0.013 μM respectively. 4-Quinazolinone analogs, MJ-68 and MJ-78, were much less effective. Using Western blotting and FACS analyses, we found that 6–12 h of MJ-66 treatment significantly increased the percentage of cells in the G2/M phase (Fig. 2A). In addition, 12 h after MJ-66 treatment, the percentage of cells in the sub-G1 phase and with DNA content >4N were significantly increased (Fig. 2B). The expression of cleaved caspase-2 and caspase-3 and the percentage of FITC$^+$/PI$^-$ cell population increased significantly after treatment of MJ-66 both *in vitro* C6 glioma cells and in vivo xenograft tumors treated with MJ-66. These data suggest that MJ-66 induces glioma cell death early through (1) G2/M arrest and mitotic catastrophe and (2) caspase-dependent apoptosis in a small population of cells.

In the present study, we found MJ-66 inhibited cell viability of rat normal glia cells with IC$_{50}$ similar to those of glioma cell lines. However, in glia cells treated with Ara-C to inhibit proliferation, MJ-66 did not induce cell death. This result suggests that proliferating cells are more sensitive to MJ-66 and MJ-66 may cause less toxicity to normal glia cells. However, glia cells proliferate constantly, this conclusion requires further verification in animal studies.

Mitotic catastrophe has been defined as a 'prestage' to necrosis or to caspase-dependent and caspase-independent apoptosis (Vakifahmetoglu et al., 2008; Mansilla et al., 2006). In contrast to our report in glioma cells, MJ-66 (previously termed HL-66)-induced mitotic

catastrophe preceded caspase-independent mode of death in skin cancer M21 cells, as indicated by the lack of typical features of apoptosis (the cell population of early and late apoptosis) by annexin V/propidium iodide staining and flow cytometry analysis (Wu et al., 2011). The differential cell death produced by MJ-66 in these studies is not clear, although MJ induced cell cycle arrest at G2/M phase in both cell lines. It is likely that the mode of MJ-66-induced cell death depends on the genetic background in the cells being treated and the concentration of drug used (Portugal et al., 2010). Previous study used 33 nM MJ-66 (Wu et al., 2011) (as opposed to 60 nM in the present study) and therefore failed to observe the late apoptosis.

Progression from G2 to M phase is driven by the activation of the Cdk1/cyclin B1 complex. The Cdk1/cyclin B1 heterodimer induces mitosis by phosphorylating and activating enzymes that regulate chromatin condensation, nuclear membrane breakdown, mitosis-specific microtubule reorganization and the actin cytoskeleton allowing for mitotic rounding up of the cell (Nigg, 2001; Castedo et al., 2004a,b). Aberrant mitotic entry, before the completion of DNA replication, can cause mitotic catastrophe and it has been suggested that premature entry of active Cdk1/cyclin B1 complex into the nucleus results in premature chromatin condensation and apoptosis (Heald et al., 1993; Fotedar et al., 1995; Jin et al., 1998; Porter et al., 2003). In the present study, we found that the expression of cyclin B1 and Cdk1 increased at 6, 12 and 18 h after the treatment with MJ-66 and then returned to baseline at 24 h. On the other hand, the phosphorylation of Cdk1 on Tyr[15] which inhibits its activity increased transiently at 6 h after the treatment with MJ-66 and then returned to baseline at 12 h. These results were consistently with the idea that MJ-66-induced glioma mitotic catastrophe was mediated through interrupting with cylin B1/Cdk1 complex activity.

In the G1 checkpoint, cyclin E and its partner Cdk2 regulate cell cycle progression. We found that expression of Cdk2 markedly increased 6 h and returned to baseline 24 h after treatment with MJ-66. This result suggests that MJ-66 is able to induce the degradation of cyclin D1 and increase in Cdk2 expression, leading to the cell cycle arrest in S phase.

BAD, a distant member of the BCL-2 family, exerts its death-promoting effect by hetero-dimerizing with BCL-X_L and BCL-2 death antagonists in the mitochondria (Yang et al., 1995). Upon phosphorylation, BAD dissociates from BCL-X_L and is bound and sequestered in the cytoplasm by the tau form of 14-3-3 proteins (Zha et al., 1996). In the present study, we found the phosphorylation of BAD at Ser112 was significantly decreased after 12 h of MJ-66 treatment. This reduces the interaction between phosphorylated Ser112 and 14-3-3, allowing BAD to translocate to mitochondria and induce cell death.

In summary, we have provided evidence for the occurrence of mitotic catastrophe and its role in glioma cells in response to MJ-66. These results coupled to inhibition of tumor growth in a xenograft animal model makes MJ-66 a promising agent for the treatment of malignant gliomas.

Acknowledgment

References

Andree HA, Reutelingsperger CP, Hauptmann R, Hemker HC, Hermens WT, Willems GM. Binding of vascular anticoagulant alpha (VAC alpha) to planar phospholipid bilayers. J. Biol. Chem. 1990; 265:4923–4928. [PubMed: 2138622]

Broker LE, Kruyt FA, Giaccone G. Cell death independent of caspases: a review. Clin. Cancer Res. 2005; 11:3155–3162. [PubMed: 15867207]

Cao SL, Feng YP, Zheng XL, Jiang YY, Zhang M, Wang Y, Xu M. Synthesis of substituted benzylamino- and heterocyclylmethylamino carbodithioate derivatives of 4-(3H)-quinazolinone and their cytotoxic activity. Arch. Pharm. 2006; 339:250–254.

Casciola-Rosen L, Rosen A, Petri M, Schlissel M. Surface blebs on apoptotic cells are sites of enhanced procoagulant activity: implications for coagulation events and antigenic spread in systemic lupus erythematosus. Proc. Natl. Acad. Sci. U. S. A. 1996; 93:1624–1629. [PubMed: 8643681]

Castedo M, Perfettini JL, Roumier T, Andreau K, Medema R, Kroemer G. Cell death by mitotic catastrophe: a molecular definition. Oncogene. 2004a; 23:2825–2837. [PubMed: 15077146]

Castedo M, Perfettini JL, Roumier T, Valent A, Raslova H, Yakushijin K, et al. Mitotic catastrophe constitutes a special case of apoptosis whose suppression entails aneuploidy. Oncogene. 2004b; 23:4362–4370. [PubMed: 15048075]

Chakrabarti A, Chakrabarti S. High yield of micronuclei and micronuclei premature chromosome condensation in a mouse tumor cell line cultured in vivo with prearrested mitotic metaphases. Neoplasma. 1987; 34:557–562. [PubMed: 3696297]

Chinigo GM, Paige M, Grindrod S, Hamel E, Dakshanamurthy S, Chruszcz M, Minor W, Brown ML. Asymmetric synthesis of 2,3-dihydro-2-arylquinazolin-4-ones: methodology and application to a potent fluorescent tubulin inhibitor with anticancer activity. J. Med. Chem. 2008; 51:4620–4631. [PubMed: 18610995]

de Bruin EC, Medema JP. Apoptosis and non-apoptotic deaths in cancer development and treatment response. Cancer Treat. Rev. 2008; 34:737–749. [PubMed: 18722718]

De Souza CP, Osmani SA. Mitosis, not just open or closed. Eukaryot. Cell. 2007; 6:1521–1527. [PubMed: 17660363]

Fotedar R, Flatt J, Gupta S, Margolis RL, Fitzgerald P, Messier H, et al. Activation-induced T-cell death is cell cycle dependent and regulated by cyclin B. Mol. Cell. Biol. 1995; 15:932–942. [PubMed: 7823958]

Fragkos M, Beard P. Mitotic catastrophe occurs in the absence of apoptosis in p53-null cells with a defective G1 checkpoint. PloS One. 2011; 6:e22946. [PubMed: 21853057]

Fukasawa K. Oncogenes and tumour suppressors take on centrosomes. Nat. Rev. Cancer. 2007; 7:911–924. [PubMed: 18004399]

Giri RS, Thaker HM, Giordano T, Chen B, Nuthalapaty S, Vasu KK, Sudarsanam V. Synthesis and evaluation of quinazolinone derivatives as inhibitors of NF-kappaB, AP-1 mediated transcription and eIF-4E mediated translational activation: inhibitors of multi-pathways involve in cancer. Eur. J. Med. Chem. 2010; 45:3558–3563. [PubMed: 20557982]

Heald R, McLoughlin M, McKeon F. Human wee1 maintains mitotic timing by protecting the nucleus from cytoplasmically activated Cdc2 kinase. Cell. 1993; 74:463–474. [PubMed: 8348613]

Hermisson M, Klumpp A, Wick W, Wischhusen J, Nagel G, Roos W, Kaina B, Weller M. O6-methylguanine DNA methyltransferase and p53 status predict temozolomide sensitivity in human malignant glioma cells. J. Neurochem. 2006; 96:766–776. [PubMed: 16405512]

Hirose Y, Berger MS, Pieper RO. p53 effects both the duration of G2/M arrest and the fate of temozolomide-treated human glioblastoma cells. Cancer Res. 2001; 61:1957–1963. [PubMed: 11280752]

Hour MJ, Huang LJ, Kuo SC, Xia Y, Bastow K, Nakanishi Y, Hamel E, Lee KH. 6-Alkylamino and 2,3-dihydro-3'-methoxy-2-phenyl-4-quinazolinones and related compounds: their synthesis, cytotoxicity and inhibition of tubulin polymerization. J. Med. Chem. 2000; 43(23):4479–4487. [PubMed: 11087572]

Hour MJ, Lee KH, Chen TL, Lee KT, Yu, Zhao, Lee HZ. Molecular modelling, synthesis, cytotoxicity and anti-tumour mechanisms of 2-aryl-6-substituted quinazolinones as dual-targeted anti-cancer agents. Br. J. Pharmacol. 2013; 169:1574–1586. [PubMed: 23638624]

Jin P, Hardy S, Morgan DO. Nuclear localization of cyclin B1 controls mitotic entry after DNA damage. J. Cell Biol. 1998; 141:875–885. [PubMed: 9585407]

Jordan MA, Wendell K, Gardiner S, Derry WB, Copp H, Wilson L. Mitotic block induced in HeLa cells by low concentrations of paclitaxel (Taxol) results in abnormal mitotic exit and apoptotic cell death. Cancer Res. 1996; 56:816–825. [PubMed: 8631019]

Kroemer G, Galluzzi L, Vandenabeele P, Abrams J, Alnemri ES, Baehrecke EH, et al. Classification of cell death: recommendations of the Nomenclature Committee on Cell Death 2009. Cell Death Differ. 2009; 16:3–11. [PubMed: 18846107]

Li HZ, He HY, Han YY, Gu X, He L, Qi QR, Zhao YL, Yang L. A general synthetic procedure for 2-chloromethyl-4(3H)-quinazolinone derivatives and their utilization in the preparation of novel anticancer agents with 4-anilinoquinazoline scaffolds. Molecules. 2010; 15:9473–9485. [PubMed: 21178902]

Lock RB, Stribinskiene L. Dual modes of death induced by etoposide in human epithelial tumor cells allow Bcl-2 to inhibit apoptosis without affecting clonogenic survival. Cancer Res. 1996; 56:4006–4012. [PubMed: 8752171]

Mansilla S, Priebe W, Portugal J. Mitotic catastrophe results in cell death by caspase-dependent and caspase-independent mechanisms. Cell Cycle. 2006; 5:53–60. [PubMed: 16319532]

Marzaro G, Guiotto A, Chilin A. Quinazoline derivatives as potential anticancer agents: a patent review (2007–2010). Expert Opin. Ther. Pat. 2012; 22:223–252. [PubMed: 22404097]

Maton, AHJ.; LaHart, S.; Quon Warner, D.; Wright, M.; Jill, D. Cells: Building Blocks of Life. New Jersey: Prentice Hall; 1997. p. 70-74.

Merritt AJ, Allen TD, Potten CS, Hickman JA. Apoptosis in small intestinal epithelial from p53-null mice: evidence for a delayed, p53-independent G2/M-associated cell death after gamma-irradiation. Oncogene. 1997; 14:2759–2766. [PubMed: 9190891]

Mosmann T. Rapid colorimetric assay for cellular growth and survival: application to proliferation and cytotoxicity assays. J. Immunol. Methods. 1983; 65:55–63. [PubMed: 6606682]

Nigg EA. Mitotic kinases as regulators of cell division and its checkpoints. Nat. Rev. Mol. Cell Biol. 2001; 2:21–32. [PubMed: 11413462]

Porter LA, Cukier IH, Lee JM. Nuclear localization of cyclin B1 regulates DNA damage-induced apoptosis. Blood. 2003; 101:1928–1933. [PubMed: 12424202]

Portugal J, Mansilla S, Bataller M. Mechanisms of drug-induced mitotic catastrophe in cancer cells. Curr. Pharm. Des. 2010; 16:69–78. [PubMed: 20214619]

Roninson IB, Broude EV, Chang BD. If not apoptosis, then what? Treatment-induced senescence and mitotic catastrophe in tumor cells. Drug Resist. Updat. 2001; 4:303–313. [PubMed: 11991684]

Vakifahmetoglu H, Olsson M, Zhivotovsky B. Death through a tragedy: mitotic catastrophe. Cell Death Differ. 2008; 15:1153–1162. [PubMed: 18404154]

Vitale I, Galluzzi L, Castedo M, Kroemer G. Mitotic catastrophe: a mechanism for avoiding genomic instability. Nat. Rev. Mol. Cell Biol. 2011; 12:385–392. [PubMed: 21527953]

Wu YC, Hour MJ, Leung WC, Wu CY, Liu WZ, Chang YH, et al. 2-(Naphthalene-1-yl)-6-pyrrolidinyl-4-quinazolinone inhibits skin cancer M21 cell proliferation through aberrant expression of microtubules and the cell cycle. J. Pharmacol. Exp. Ther. 2011; 338:942–951. [PubMed: 21652781]

Yang E, Zha J, Jockel J, Boise LH, Thompson CB, Korsmeyer SJ. Bad, a heterodimeric partner for Bcl-x$_L$ and Bcl-2, displaces bax and promotes cell death. Cell. 1995; 80:285–291. [PubMed: 7834748]

Zhou YH, Wu X, Tan F, Shi YX, Glass T, Liu TJ, Wathen K, Hess KR, Gumin J, Lang F, Yung WK. PAX6 suppresses growth of human glioblastoma cells. J. Neurooncol. 2005; 71:223–229. [PubMed: 15735909]

Zha J, Harada H, Yang E, Jockel J, Korsmeyer SJ. Serine phosphorylation of death agonist BAD in response to survival factor results in binding to 14-3-3 not BCL-X(L). Cell. 1996; 87:619–628. [PubMed: 8929531]
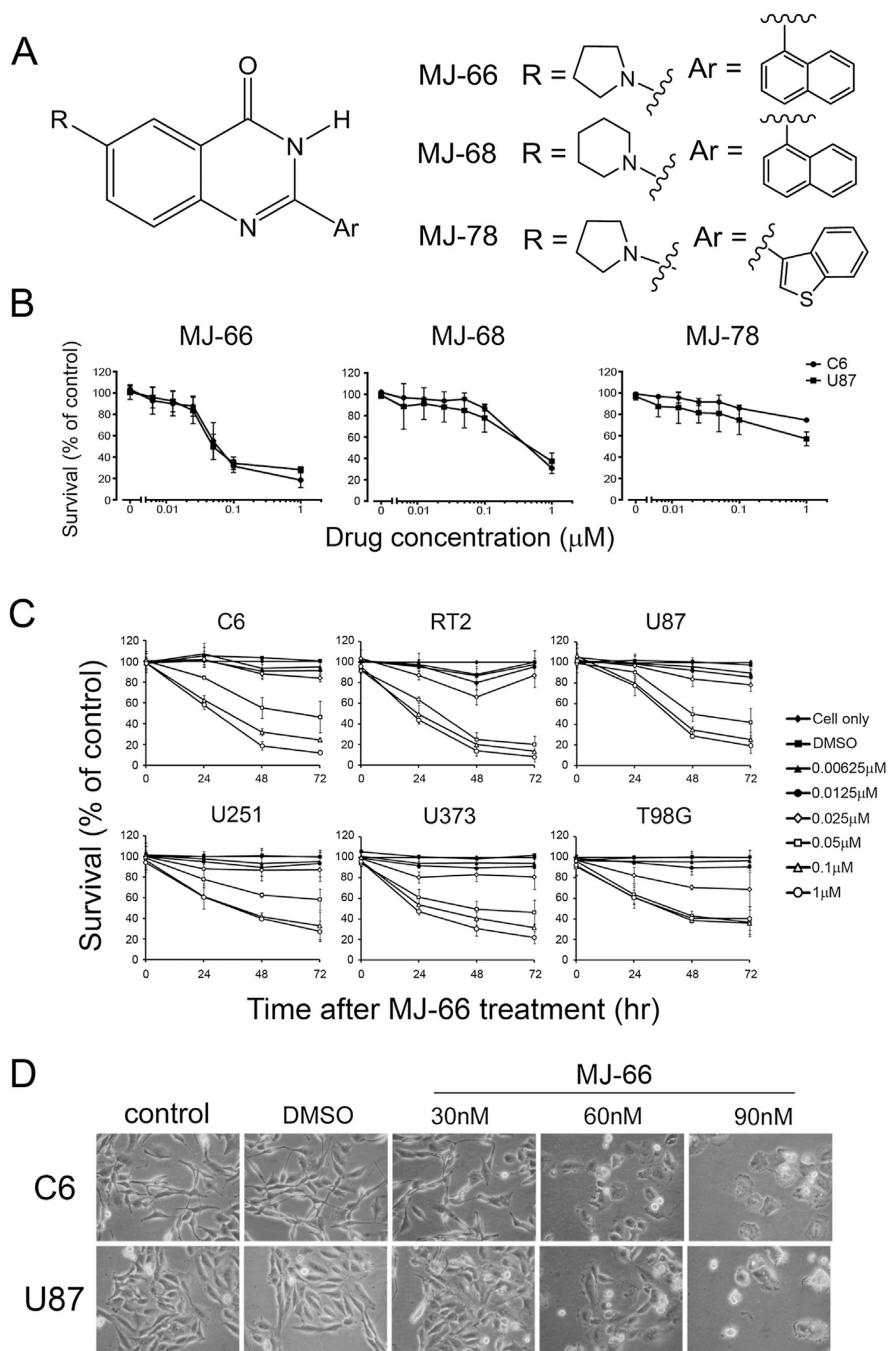
Fig. 1. Effects of quinazolinone analogs on glioma cell lines
A. The structures of MJ-66, MJ-68 and MJ-78. B. Concentration-dependent effects of MJ-66, MJ-68 and MJ-78 on C6 and U87 Glioma cell lines. Cells were treated with various concentrations of drugs for 48 h and cell viability was determined by MTS assay. C. Concentration- and time-dependent reduction of cell viability in various glioma cell lines by MJ-66. D. C6 and U87 glioma cells were treated with MJ-66 (30, 60, 90 nM) or vehicle (DMSO, 0.009%) for 48 h and morphological changes were observed including cell rounding and shrinkage.
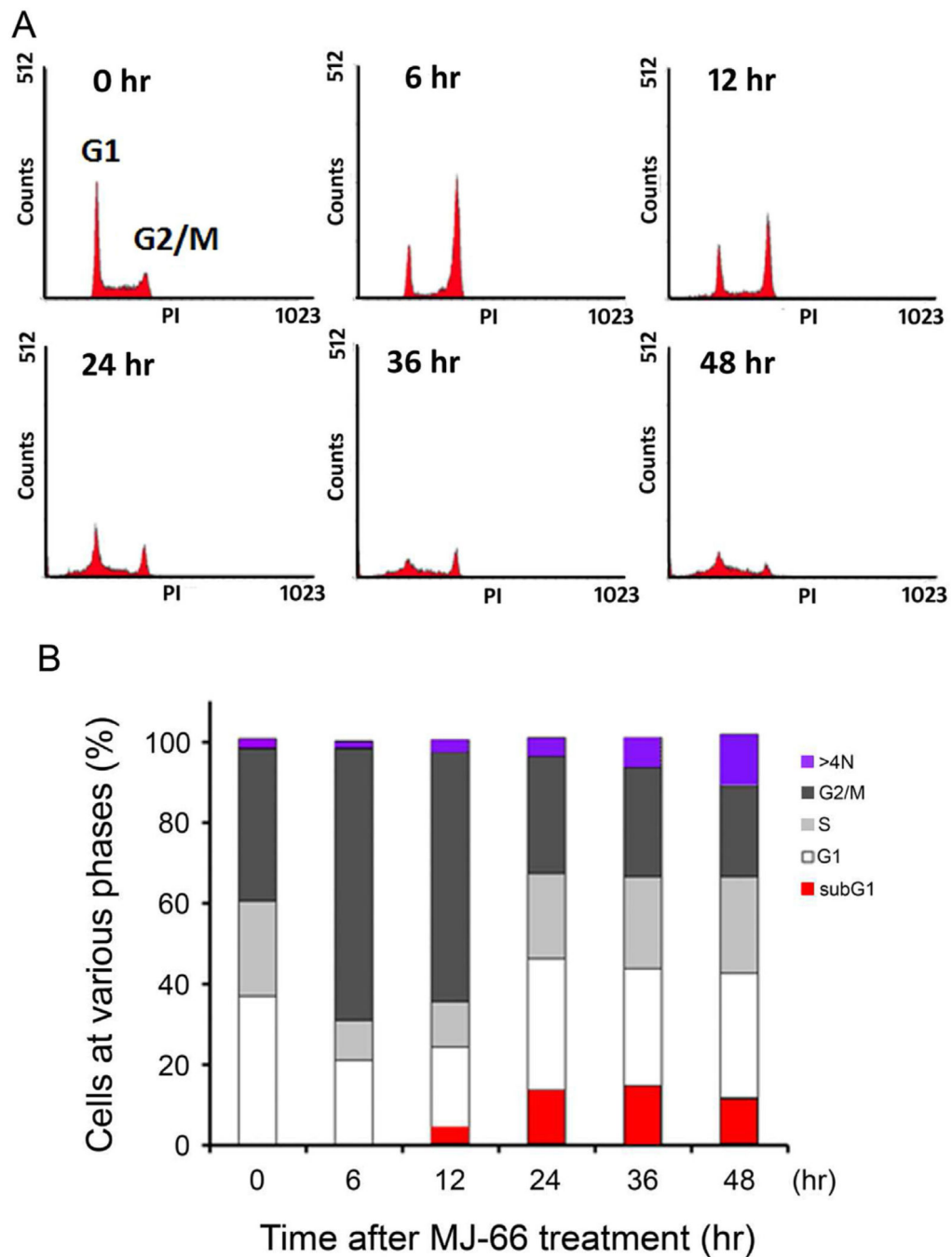
Fig. 2. MJ-66 induced glioma cells G2/M arrest and cell death
A. C6 glioma cells were treated with MJ-66 (60 nM) for the indicated times and cell cycle distributions were monitored by flow cytometry with propidium iodide staining. B. The graph displayed the percentage of subG1, G1, S, G2/M and >4N DNA content analyzed from (A).
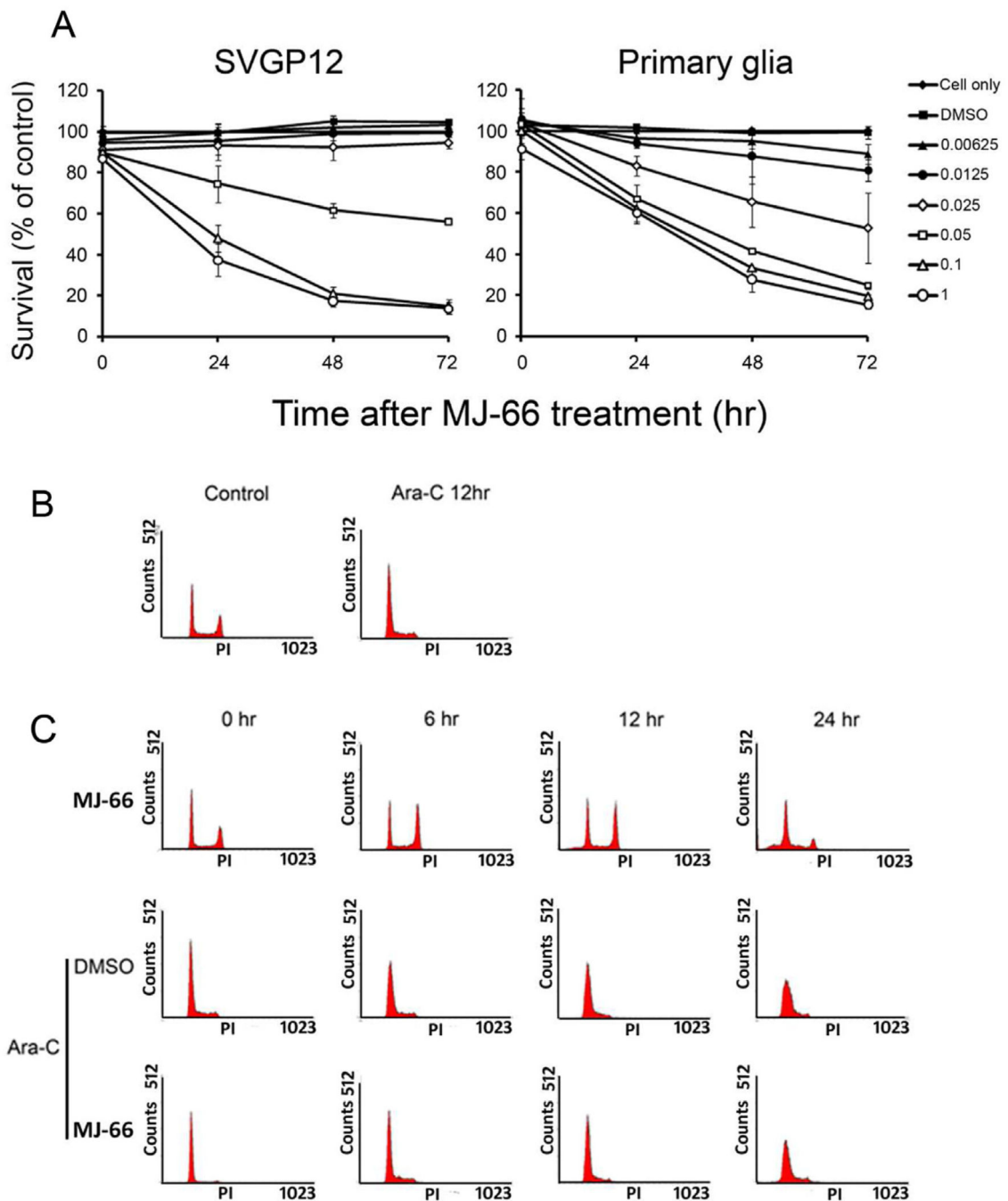
Fig. 3. MJ-66 has no effect on non-proliferating cell death

A. Concentration-dependent effects of MJ-66 on human normal glia cell line and rat primary glia cells. Cells were treated with MJ-66 at various times as indicated. B. C6 glioma cells were treated with Ara-C (41.6 nM) for the indicated times and cell cycle distributions were monitored by flow cytometry with propidium iodide staining. C. Upper panel: C6 glioma cells were treated with MJ-66 (60 nM) for the indicated times and cell cycle distributions were monitored by flow cytometry with propidium iodide staining. Middle and Lower panels: C6 glioma cells were pre-treated with Ara-C (41.6 nM) for 12 h and were treated

with MJ-66 (60 nM) for the indicated times. Cell cycle distributions were monitored by flow cytometry with propidium iodide staining.
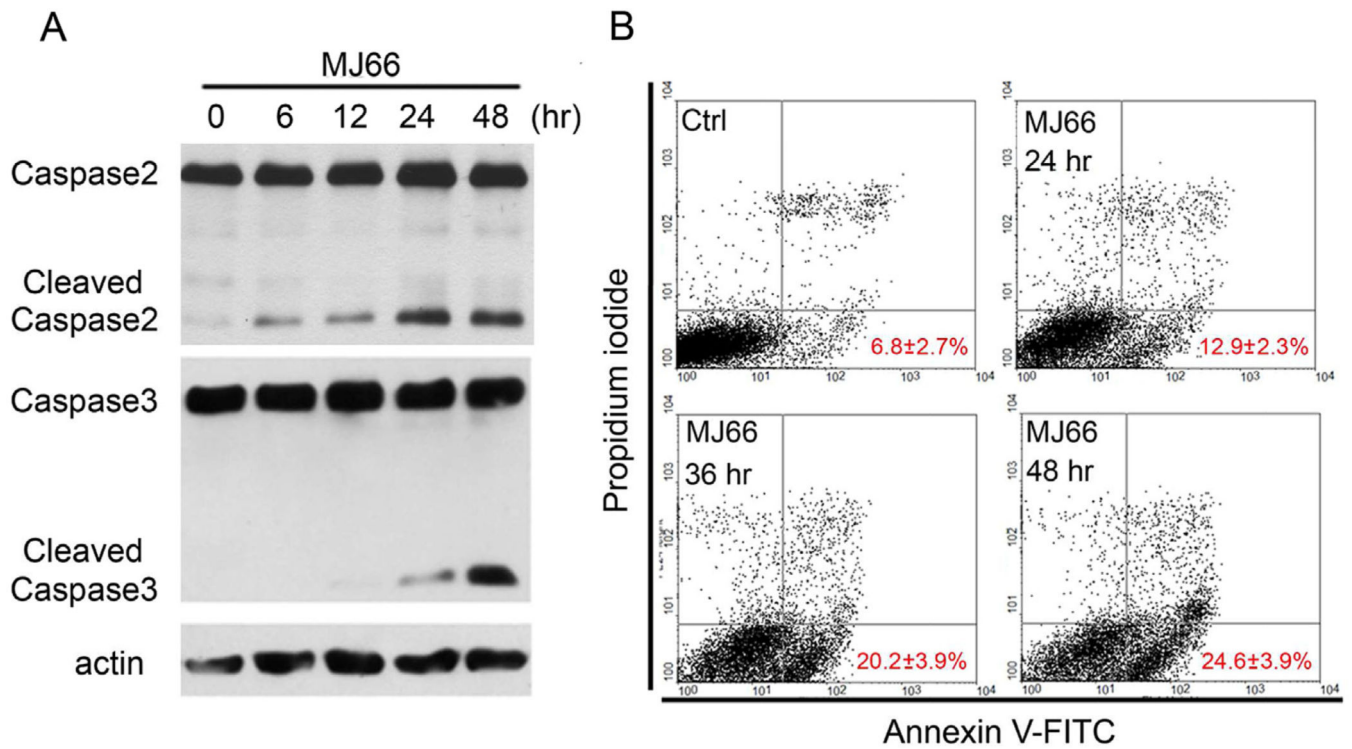
Fig. 4. MJ-66 induced glioma cells apoptosis but not necrosis

A. Western blotting analysis of caspase-2 and caspase-3 activation in U87 glioma cells treated with vehicle (DMSO) or MJ-66 (60 nM) for the indicated times. B. U87 glioma cells, treated with MJ-66 (60 nM) for the indicated times, were stained with propidium iodide and annexin V-FITC and analyzed with flow cytometry.
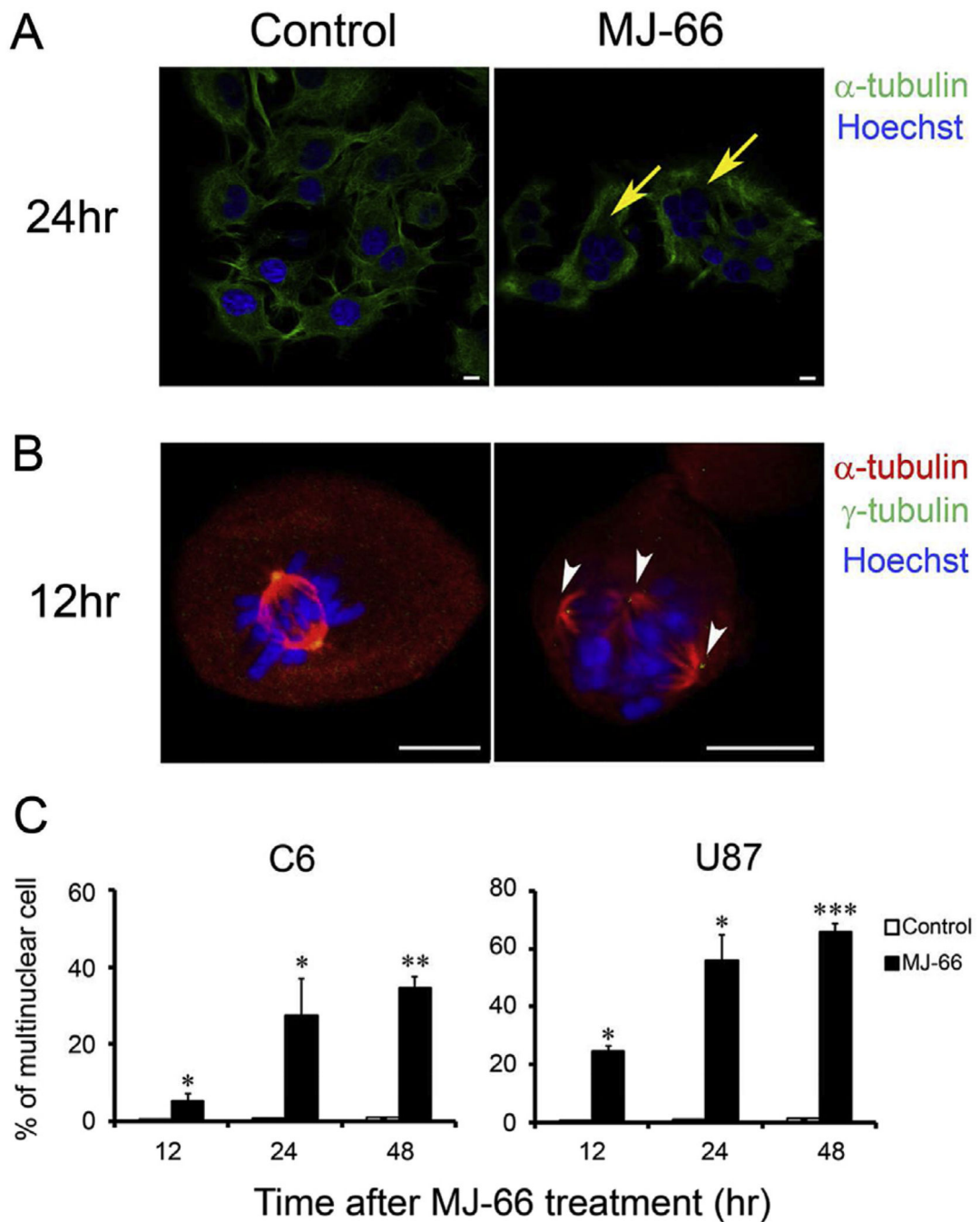
Fig. 5. MJ-66 induces multinucleated phenotype and multipolar spindles in glioma cells
A. U87 glioma cells were treated with MJ-66 (60 nM) for 24 h and were stained with Hoechst 33342 and antibody for α-tubulin (green) (arrows: multinucleated cells). Bar: 10 μm. B. U87 glioma cells were treated with MJ-66 (60 nM) for 12 h and were stained with Hoechst 33342 and antibodies for α-tubulin (red) and γ-tubulin (green) (arrow heads: multipolar spindles). Bar: 10 μm. C. Quantitative analysis of multinucleated cells after treatment with MJ-66 (60 nM) for the indicated times. $*p < 0.05$, $**p < 0.01$, $***p < 0.001$

vs. DMSO. (For interpretation of the references to color in this figure legend, the reader is referred to the web version of this article.)
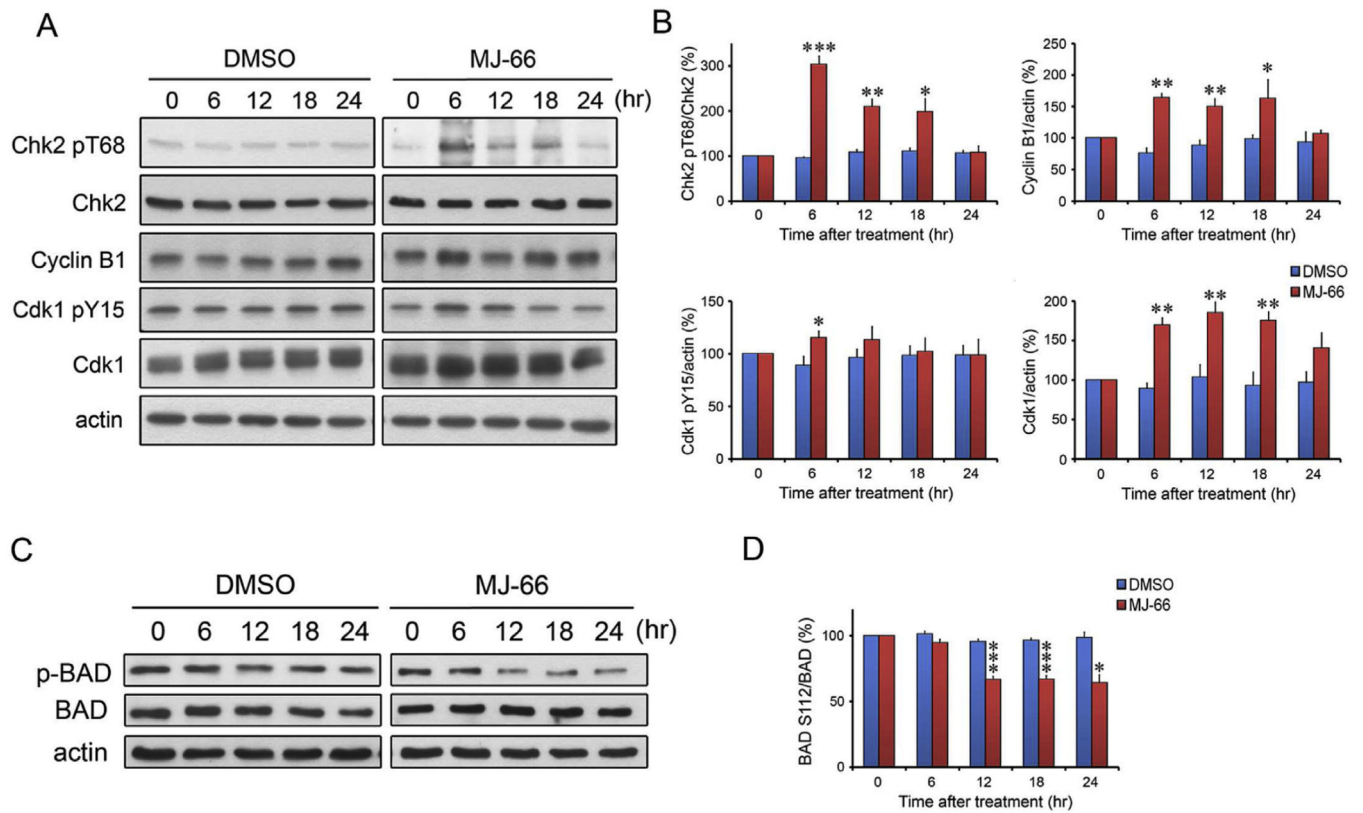
Fig. 6. MJ-66 increases Chk2/Cdk1/cyclin B1 activity and phosphorylation of BAD in C6 glioma cells

A & B. C6 glioma cells were treated with MJ-66 (60 nM) or vehicle (DMSO) for indicated times and cell lysates were blotted with Chk2 pT68, Cyclin B1, Cdk1 pY15 and Cdk1. C & D. C6 glioma cells were treated with MJ-66 (60 nM) or vehicle (DMSO) for indicated times and cell lysates were blotted with BAD pS112 and BAD.*$p < 0.05$, **$p < 0.01$, ***$p < 0.001$ vs. DMSO.
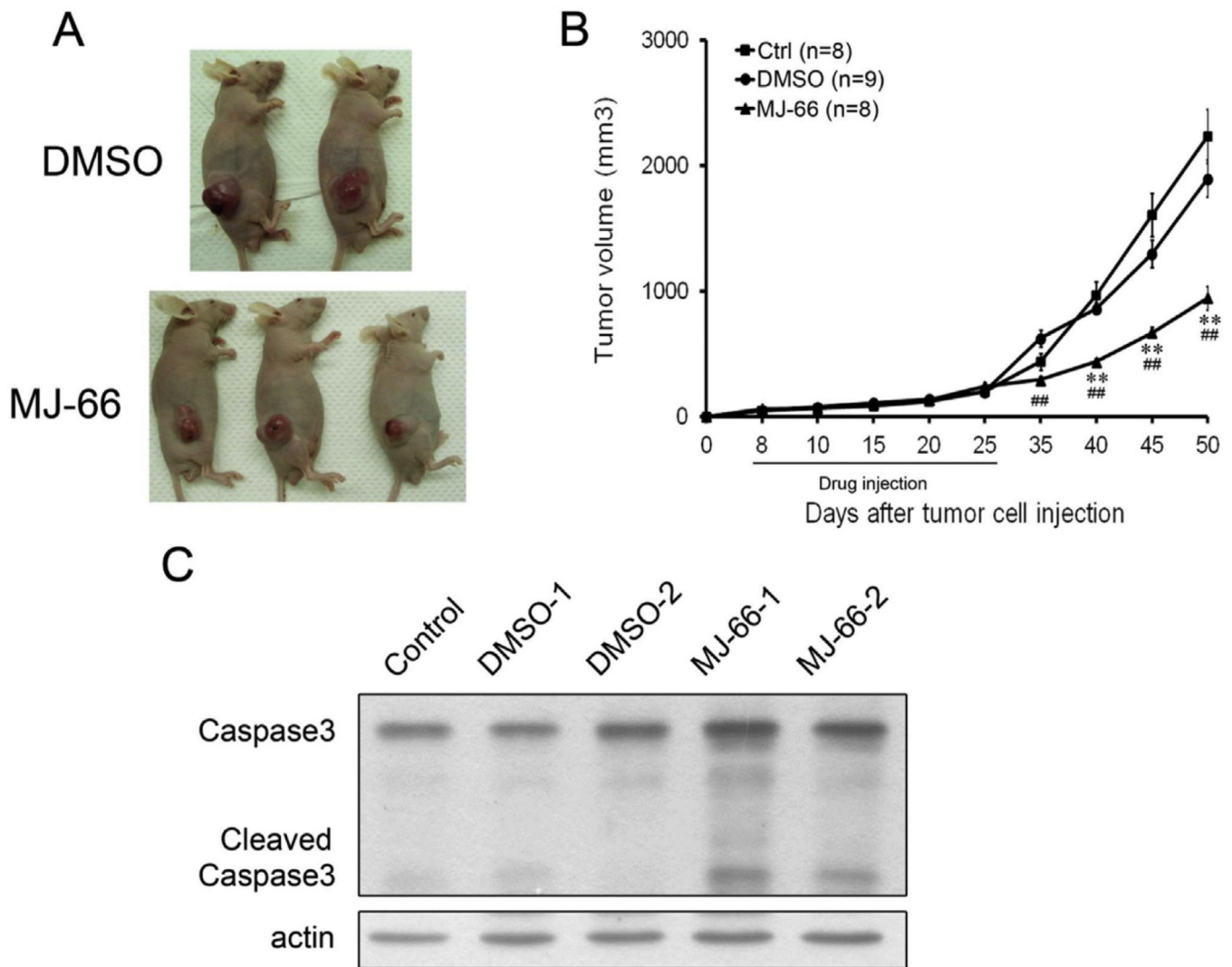
Fig. 7. MJ-66 inhibits tumor growth in a xenograft animal model
A & B. U87 glioma cells (1×10^6) were inoculated subcutaneously into the nude mice ($n = 6$ for each group). When the tumors reached 50–70 mm^3 in volume, intraperitoneal injections of MJ-66 (1.36 μg/kg) were administered every 48 h for 10 times and tumor volume was measured for another 30 days after the cessation of treatment. C. Western blots showed induction of caspase-3 activation at 30 days after the cessation of treatment.

Table 1

The IC_{90}, IC_{50} and IC_{10} of C6 and U87 glioma cell line treated with quinazolinone analogs at 48 h.

	Cell line	IC_{90} (μM)	IC_{50} (μM)	IC_{10} (μM)
MJ-66	C6	>1	0.06 ± 0.015	0.02 ± 0.010
	U87	>1	0.55 ± 0.013	0.02 ± 0.009
MJ-68	C6	>1	0.47 ± 0.165	0.08 ± 0.016
	U87	>1	0.57 ± 0.240	0.06 ± 0.068
MJ-78	C6	>1	>1	0.05 ± 0.027
	U87	>1	>1	0.04 ± 0.039

IC_{90} represents the inhibitory concentration that reduces 90% cell survival; IC_{50} represents the inhibitory concentration that reduces 50% cell survival; IC_{10} represents the inhibitory concentration that reduces 10% cell survival.

Table 2

IC$_{90}$, IC$_{50}$ and IC$_{10}$ of several glioma cell lines and normal glia cells treated with MJ-66 at 48 h.

	IC$_{90}$ (μM)	IC$_{50}$ (μM)	IC$_{10}$ (μM)
C6	>1	0.06 ± 0.015	0.02 ± 0.010
U87	>1	0.05 ± 0.013	0.02 ± 0.009
RT2	>1	0.04 ± 0.004	0.01 ± 0.001
U373	>1	0.06 ± 0.024	0.02 ± 0.008
U251	>1	0.08 ± 0.006	0.02 ± 0.013
T98G	>1	0.05 ± 0.005	0.01 ± 0.004
SVGP12	>1	0.06 ± 0.002	0.03 ± 0.006
Glia	>1	0.04 ± 0.010	0.01 ± 0.006

IC$_{90}$ represents the inhibitory concentration that reduces 90% cell survival; IC$_{50}$ represents the inhibitory concentration that reduces 50% cell survival; IC$_{10}$ represents the inhibitory concentration that reduces 10% cell survival.